Journal of Petroleum Science and Engineering 127 (2015) 137–147

Contents lists available at ScienceDirect

Journal of Petroleum Science and Engineering

journal homepage: www.elsevier.com/locate/petrol

A computational analysis for quantitative evaluation of petrol-physical properties of rock fluids based on Bloch NMR diffusion model for porous media

O.M. Dada, O.B. Awojoyogbe *, A.C. Ukoha

Department of Physics, Federal University of Technology, P.M.B. 65, Minna 920001, Niger State, Nigeria

ARTICLE INFO

Article history:
Received 21 May 2014
Accepted 9 January 2015
Available online 2 February 2015

Keywords:
Bloch NMR flow equation
complex lithology
porosity
tortuosity
petro-physics

ABSTRACT

Estimating permeability from grain-size distributions or from well logs is attractive but very difficult. The difficulties are inherent in many petroleum-bearing reservoirs and complex mineralogy earth formations where existing nuclear magnetic resonance (NMR) models require modifications to work effectively. In this paper, we present a generally applicable and simple approach which may yield useful information from NMR signals of different petro-physical properties and porosity. This approach is a model of the Bloch NMR diffusion equation for complex pore geometries in which the transverse magnetization is obtained as function of reservoir chemical (relaxation) and physical properties. The NMR signal is also shown to be dependent on the tortuosity and relaxation rate of rocks fluid so that reservoirs comprised of mixed lithology and mineralogy can be easily evaluated. The computational tools obtained in this study are useful for repetitive data processing which is otherwise difficult due to hardware limitations and logistic issues.

© 2015 Elsevier B.V. All rights reserved.

1. Introduction

The introduction of pulsed NMR logging tools in the early 1990s provided the oil and gas industry with powerful new methods for evaluating petroleum reservoirs (Freedman and Heaton, 2004). NMR measurements are based on three NMR physical principles (Chen et al., 2011): (i) the proportionality of the proton NMR signal strength to the fluid volume in the voids (that is, pore spaces) of the porous rock, (ii) the relationship of the wetting-phase fluid relaxation time to the individual pore dimensions and (iii) the use of relaxation times and diffusion contrasts among the fluid phases to discern reservoir fluids and non-native fluids, such as drilling fluids filtrating to the rock. The use of NMR for logging experiment and for porous media in general is because relaxation rates ($1/T_1$ and $1/T_2$) are very sensitive to the interactions between protons in rock fluids and the surrounding pore walls (Howard, 1998).

The spatial resolution attainable in heterogeneous porous rocks is inherently limited because of the magnetic susceptibility contrast between solid and fluid flowing within rock pores (Mitchell et al., 2013). This is the reason why imaging resolution better than typical pore diameters is not practical and hence, MRI of core-plugs has often been considered to be an inappropriate use of expensive magnetic resonance facilities. However, in recent practice, there has been a change in the use of MRI in laboratory-scale rock core analysis (Mitchell et al., 2013). Acquisition of data in the laboratory which are directly comparable to data obtained from magnetic resonance well-logging tools (that is, a common physics of measurement) is now the order of the day. Well-logging tools operate at very low magnetic field strengths and usually equivalent low-field benchtop magnets are typically supplied with magnetic field gradient coils for diffusion measurements and so one-dimensional images (profiles) are readily obtainable (Mitchell et al., 2013). Magnetic resonance has proved to be very useful within the petrophysical community in the form of well-logging tools: a single-sided permanent magnet and radio frequency (RF) resonator are lowered into a well in order to investigate the fluid properties in the formation near the bore (Mitchell et al., 2013).

The recovery of oil from reservoirs has been the motivation behind the current research efforts in NMR logging (Mitchell et al., 2013). The properties of both the fluids (oil, water or brine, miscible or immiscible gas) present in the reservoir and the rock matrix (pore network, mineral composition and their mechanical performance) need to be assessed in order to predict remaining oil reserves and potential recovery accurately (Mitchell et al., 2013). However, new petroleum resources are often found in complex-lithology formations (Chen et al., 2011). Rocks with complex lithology formations are often highly heterogeneous in texture, mineral composition/distribution, and pore and grain sizes (Chen et al., 2011; Mitchell

* Correspondence author.
E-mail addresses: awojoyogbe@yahoo.com, abamidele@futminna.edu.ng (O.B. Awojoyogbe).

http://dx.doi.org/10.1016/j.petrol.2015.01.003
0920-4105/© 2015 Elsevier B.V. All rights reserved.

et al., 2013). Physical and chemical changes can accompany the deposition of the sediments and/or post-depositional diagenetic process of the rocks. These changes show different NMR responses to the fluids (such as oil, water and gas) which are found within the pore spaces.

The hydrogen nuclei contained in the oil, gas, and brine filling the rock pore spaces behaves like microscopic magnets or spins (Freedman and Heaton 2004; Coates et al., 1999). The magnetic moments of the hydrogen nuclei align along the direction of the applied magnetic field create a net magnetization or polarization in the formation. The time required to align the hydrogen nuclei along the direction of the applied magnetic field, referred to as the longitudinal direction, is characterized by a longitudinal relaxation time denoted by T_1 (Freedman and Heaton 2004) while the interactions between bulk and pore fluids are characterized by the transverse relaxation time T_2 (Morriss et al., 1994). In practice, a distribution of T_1s is required to describe the magnetization process. The distributions reflect the complex composition of crude oils and the distribution of pore sizes in sedimentary rocks. For bulk crude oils, the logarithmic mean of the T_1 distribution is inversely proportional to the viscosity and can vary from a few milliseconds or less for heavy oils to several seconds for low-viscosity oils (Freedman and Heaton, 2004). The equation of motion of the spins filling the rock spaces in the presence of B_0 and B_1 is the Bloch NMR equation. In the presence of flow in pore spaces with relatively slow fluid diffusion, the NMR diffusion equation (Awojoyogbe et al., 2011; Gupta et al., 2014) is employed for the evaluation of the NMR transverse magnetization (M_y) as a function of reservoir relaxation and morphological features.

According to pore structure, oil- or water-bearing (reservoir) rocks can be classified as cylindrical pore system as shown in Fig. 1. They are examples of porous materials (often called matrix) which are generally permeated by interconnected network of pores (voids) filled with a fluid. The understanding of the important properties of this materials, such as porosity, could reveal the nature of fluid pore geometry, the permeability, and hence, the fluid they contain, and the molecular interaction between the fluid particles and the surface of the pores.

A porous medium is most often characterized by its porosity. Other properties of the medium (such as permeability, tensile strength, and electrical conductivity) can sometimes be derived from the respective properties of its constituents (solid matrix and fluid) and the media porosity and pores structure, though the derivation is usually complex, many of the important properties of oil- or water-bearing (reservoir) rocks can only be rationalized by considering them to be porous media.

Based on the NMR diffusion equation (Awojoyogbe et al., 2011; Gupta et al., 2014), NMR logging data can offer an improved method, which may be used independently or in combination with conventional logging data, to determine reservoir properties. In some complex environments (e.g. mixed-lithology reservoirs, low-resistivity/low-contrast pay zones, low-porosity/low permeability formations, and medium-to-heavy oil reservoirs), where conventional logging tools may fail to unveil important reservoir properties, NMR may be the only technique available to assess them. Reliable and accurate NMR measurements of these reservoir properties require careful early job planning. Such planning is critical for the success of the logging run. Specific formation and fluid properties can be utilized to design an acquisition scheme that provides access to yet unknown reservoir characteristics and that optimizes the acquisition process and thus improves the answers derived from the data. If acquisition parameters are not selected properly, answer products may provide properties that differ significantly from the actual reservoir properties (Mitchell et al., 2013; Coates et al., 1999). Magnetic Resonance Imaging Logging (MRIL) job planning can be executed in three basic steps: (i) Determine NMR fluid properties ($T_{1,bulk}$, $T_{2,bulk}$, D_0, and HI). (ii) Assess expected NMR responses (decay spectrum, polarization, apparent porosity) over the intervals to be logged. (iii) Select activation sets and determine appropriate activation parameters (TW, TE, NE) (Coates et al., 1999).

Within the laboratory, NMR is a powerful technique that gives information on fluids confined in porous materials (Mitchell et al.,

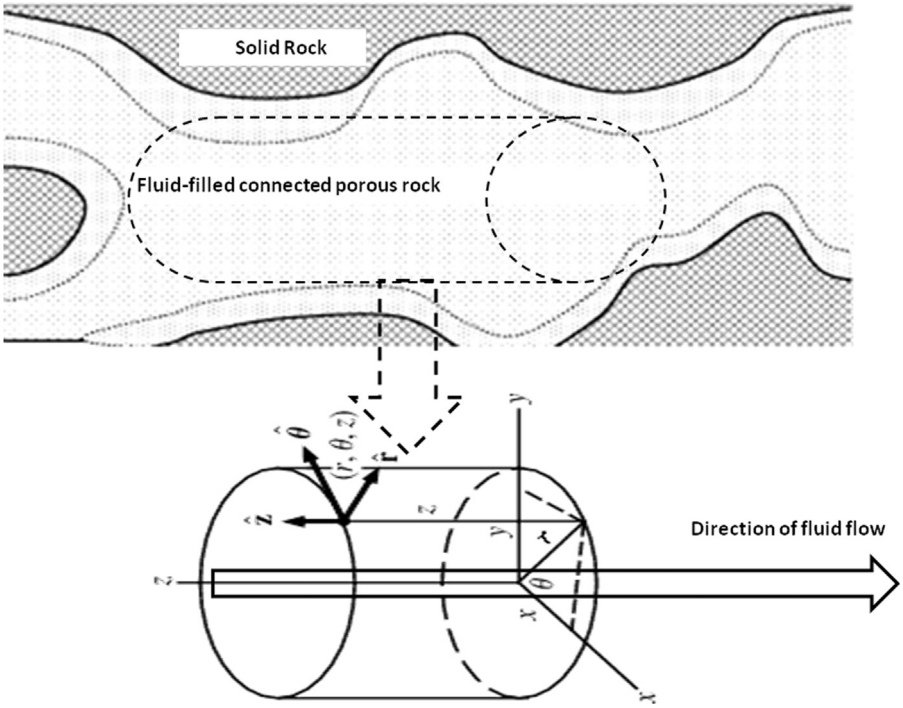

Fig. 1. A fluid-filled connected porous rock modelled as a cylindrical pore system (Sen, 2004).

2013). Understanding of oil recovery processes in laboratory experiments is crucial for generating accurate models to predict field-scale performance in the petroleum reservoir (Mitchell et al., 2013; Kleinberg et al., 1994). The field of NMR which addresses this measurement is normally regarded as time domain analysis which encompasses spin relaxation and diffusion. Time domain analysis may be combined with other methods in a single measurement (Mitchell et al., 2013), although the hardware requirements of the acquisition sequences can be very different depending on the application.

However, in the application of NMR theory to complex lithologies, heterogeneities in the pore sizes have been quite challenging (Kleinberg et al., 1994) because the composition of pore materials is difficult to be thoroughly characterized (Kleinberg et al., 1994). In fact, NMR sequences for data acquisition are usually designed to fit mostly to particular systems and applications (Gupta et al., 2014); this places limitations on imaging of porous rocks with nonlinear behaviour. Acquisition of relaxation data requires the use of different NMR pulse sequences, each of which is time-consuming. When the petrophysicist is required to perform repetitive investigations, the task becomes quite cumbersome. In the presence of straightforward computational tool, the researcher may only need few data to get necessary information in preparation for a detailed experimental investigation. It gives the opportunity to predict fluid/pore behaviour, run the data several times within a relatively short time and interpolate for data combinations which are not possible on the hardware. Also, sensitivity to spatial variations in porosity and fluid saturation is very necessary for encoding other parameters in the images (Mitchell et al., 2013) such as chemical shift (spectroscopy), relaxation time, or diffusion coefficient; when the tortuosity is included, we may be able to monitor how twisted the rock pores are.

In order to develop such a computational tool, we present a model of the Bloch NMR diffusion equation for quantitative analyses of complex pore geometries in which the transverse magnetization is obtained as a function of reservoir chemical (relaxation) and petrol-physical properties which can be very important for job planning and for interpreting complicated logs.

2. Theoretical formulation

The borehole and laboratory NMR measurements described above aim at determining the magnetization and relaxation times of the protons in the bulk and pore fluid (Morriss et al., 1994). When diffusion processes are present, this magnetization depends on the diffusion coefficient. In our earlier studies, an important equation for the description of motion of diffusing fluid spins has been developed (Awojoyogbe et al., 2010, 2011; Gupta et al., 2014). This equation is suitable for the evaluation of NMR signal in heterogeneous formations; for cylindrical rock pores and in the presence of radiofrequency (RF) field, the NMR diffusion equation is given as follows (Awojoyogbe et al., 2010, 2011; Gupta et al., 2014):

$$\frac{\partial M_y}{\partial t}=\frac{1}{r}\frac{\partial}{\partial r}\left(D_r r\frac{\partial M_y}{\partial r}\right)+\frac{1}{r^2}\frac{\partial}{\partial \phi}\left(D_\phi\frac{\partial M_y}{\partial \phi}\right)+\frac{\partial}{\partial z}\left(D_z\frac{\partial M_y}{\partial z}\right)+\frac{F_o}{T_o}\gamma B_1(t) \tag{1}$$

Eq. (1) describes the dynamics of the transverse magnetization (M_y) of the spins within the pore of effective radii r. D_r is the diffusion coefficient in the radial direction, D_ϕ is the ϕ-dependent diffusion coefficient and D_z is the z-dependent diffusion coefficient. Since we have assumed the presence of slow diffusion, it could be said that the spatial diffusion coefficient vary very slowly with spatial coordinates such that $D\approx D_r\approx D_\phi\approx D_z$ (that is the constant diffusion coefficient). If we sample the M_y at the point where the radiofrequency (RF) field has the highest magnitude, $M_0\approx 0$. If the porous medium has a constant diffusion coefficient, D along its channels, we write (Awojoyogbe et al., 2011; Gupta et al., 2014):

$$\frac{\partial M_y}{\partial t}=D\left(\frac{\partial^2 M_y}{\partial r^2}+\frac{1}{r}\frac{\partial M_y}{\partial r}+\frac{1}{r^2}\frac{\partial^2 M_y}{\partial \phi^2}+\frac{\partial^2 M_y}{\partial z^2}\right)+\frac{F_o}{T_o}\gamma B_1(t) \tag{2}$$

where $F_o=(M_o/T_1)$, $T_g=(1/T_1T_2)$, $T_0=(1/T_1)+(1/T_2)$, D is the diffusion coefficient, γ is the gyromagnetic ratio, T_1 is the spin lattice relaxation time, T_2 is the spin–spin relaxation time, M_o is the equilibrium magnetization, RF $B_1(x, t)$ is the applied radio-frequency magnetic field and M_y is the transverse magnetization, $(1/T_1)$ is the spin lattice relaxation rate and $(1/T_2)$ is the spin–spin relaxation time.

However, since the voxel or the region in view is always very small, the same amount of RF power is always delivered to the voxel such that the position of the magnetic particle is not a factor significant enough to be considered, we may therefore write Eq. (2) as

$$\frac{\partial M_y}{\partial t}-\frac{F_o}{T_o}\gamma B_1(t)=D\left(\frac{\partial^2 M_y}{\partial r^2}+\frac{1}{r}\frac{\partial M_y}{\partial r}+\frac{1}{r^2}\frac{\partial^2 M_y}{\partial \phi^2}+\frac{\partial^2 M_y}{\partial z^2}\right) \tag{3}$$

We assume a solution of the following form (where M_{y1} and $w(t)$ are arbitrary functions used for problem simplification) (Awojoyogbe and Dada, 2011):

$$M_y(r,\phi,z,t)=M_{y1}(r,\phi,z,t)+w(t) \tag{4}$$

Eq. (1) becomes

$$\frac{1}{D}\frac{\partial M_{y1}}{\partial t}=\frac{\partial^2 M_{y1}}{\partial r^2}+\frac{1}{r}\frac{\partial M_{y1}}{\partial r}+\frac{1}{r^2}\frac{\partial^2 M_{y1}}{\partial \phi^2}+\frac{\partial^2 M_{y1}}{\partial z^2} \tag{5}$$

provided that

$$\frac{dw(t)}{dt}=\frac{F_o}{T_o}\gamma B_1(t) \tag{6}$$

If the term M_{y1} does not vary significantly with ϕ and z, we may write

$$\frac{1}{D}\frac{\partial M_{y1}}{\partial t}=\frac{\partial^2 M_{y1}}{\partial r^2}+\frac{1}{r}\frac{\partial M_{y1}}{\partial r} \tag{7}$$

A fundamental expression for the permeability (k) of a porous medium is given by the modified Kozeny–Carman equation (Pape et al., 1998):

$$k=\frac{r^2}{8F} \tag{8}$$

where r is the effective radii of the hydraulic capillary, F is the formation factor, which is defined as the ratio of tortuosity (τ) and porosity (p):

$$F=\frac{\tau}{p} \tag{9}$$

Then

$$k=\frac{r^2 p}{8\tau}$$

Within some approximation limits, the tortuosity equation has been given as (Pape et al., 1998):

$$\tau\approx\frac{0.67}{p} \tag{10}$$

Therefore, for general consideration of the tortuosity of porous rocks, we shall assume:

$$\tau=\frac{\alpha}{8p} \tag{11}$$

For a pigeon hole model of common sandstones (Pape et al., 1998), $\alpha\approx 5.36$. The parameter α is now a unique property of various types

of rocks. Eq. (8) may then be written as

$$k=\frac{r^2p^2}{\alpha} \tag{12}$$

$$p=\frac{\sqrt{\alpha k}}{r} \tag{13}$$

The transverse magnetization is proportional to the number of protons in the sensitive region and may be scaled to give porosity (Morriss et al., 1994). Hence, using Eq. (13), the effective radii-dependent transverse magnetization can be transformed (Kreyszig 1996) into a porosity dependent transverse magnetization. Therefore, from Eq. (7), we obtain

$$\frac{\partial M_{y1}}{\partial r}=\frac{\partial M_{y1}}{\partial p}\frac{dp}{dr} \tag{14}$$

$$\frac{\partial^2 M_{y1}}{\partial r^2}=\frac{\partial^2 M_{y1}}{\partial p^2}\left(\frac{dp}{dr}\right)^2+\frac{\partial M_{y1}}{\partial p}\frac{d^2p}{dr^2} \tag{15}$$

$$\frac{dp}{dr}=-\frac{\sqrt{\alpha k}}{r^2},\quad \frac{d^2p}{dr^2}=\frac{2\sqrt{\alpha k}}{r^3},\quad \left(\frac{dp}{dr}\right)^2=\frac{\alpha k}{r^4}$$

Hence, Eq. (7) becomes

$$\frac{1}{D}\frac{\partial M_{y1}}{\partial t}=\frac{\partial^2 M_{y1}}{\partial p^2}\left(\frac{dp}{dr}\right)^2+\frac{\partial M_{y1}}{\partial p}\frac{d^2p}{dr^2}+\frac{1}{r}\frac{\partial M_{y1}}{\partial p}\frac{dp}{dr} \tag{16}$$

$$\frac{1}{D}\frac{\partial M_{y1}}{\partial t}=\frac{\alpha k}{r^4}\frac{\partial^2 M_{y1}}{\partial p^2}+\frac{2\sqrt{\alpha k}}{r^3}\frac{\partial M_{y1}}{\partial p}-\frac{1}{r}\frac{\sqrt{\alpha k}}{r^2}\frac{\partial M_{y1}}{\partial p} \tag{17}$$

$$\frac{1}{D}\frac{\partial M_{y1}}{\partial t}=\frac{\alpha k}{r^4}\frac{\partial^2 M_{y1}}{\partial p^2}+\frac{\sqrt{\alpha k}}{r^3}\frac{\partial M_{y1}}{\partial p}$$

$$\frac{1}{D}\frac{\partial M_{y1}}{\partial t}=\frac{p^4}{\alpha k}\frac{\partial^2 M_{y1}}{\partial p^2}+\frac{p^3}{\alpha k}\frac{\partial M_{y1}}{\partial p} \tag{18}$$

$$\frac{\alpha k}{D}\frac{\partial M_{y1}}{\partial t}=p^4\frac{\partial^2 M_{y1}}{\partial p^2}+p^3\frac{\partial M_{y1}}{\partial p} \tag{19}$$

By the method of separation of variables, Eq. (19) can be written in the form (Kreyszig 1996)

$$M_{y1}=G(t)W(p) \tag{20}$$

$$\frac{\alpha k}{DG}\frac{dG}{dt}=\frac{p^4}{W}\frac{d^2W}{dp^2}+\frac{p^3}{W}\frac{dW}{dp} \tag{21}$$

Eq. (21) must be equal to a constant $-\beta^2$; so that we have the following equations:

$$\frac{dG}{dt}=-\frac{\beta^2 D}{\alpha k}G \tag{22}$$

$$p^4\frac{d^2W}{dp^2}+p^3\frac{dW}{dp}+\beta^2W=0 \tag{23}$$

The solution to Eq. (22) is given as (Kreyszig 1996)

$$G(t)=A_o e^{-(\beta^2 D/\alpha k)t} \tag{24}$$

where A_o is a constant. In solving Eq. (23), we shall assume:

$$p=\frac{1}{\sigma} \tag{25}$$

Following the same procedures as in Eqs. (14)–(18), we derive

$$p^4\left(\frac{1}{p^4}\frac{d^2W}{d\sigma^2}+\frac{2}{p^3}\frac{dW}{d\sigma}\right)+p^3\left(-\frac{1}{p^2}\frac{dW}{d\sigma}\right)+\beta^2W=0 \tag{26}$$

$$\frac{d^2W}{d\sigma^2}+2p\frac{dW}{d\sigma}-p\frac{dW}{d\sigma}+\beta^2W=0 \tag{27}$$

$$\frac{d^2W}{d\sigma^2}+p\frac{dW}{d\sigma}+\beta^2W=0 \tag{28}$$

$$\frac{d^2W}{d\sigma^2}+\frac{1}{\sigma}\frac{dW}{d\sigma}+\beta^2W=0 \tag{29}$$

Eq. (29) is the Bessel differential equation where W is the Bessel function of the zeroth order (Kreyszig 1996):

$$W(\sigma)=C_0J_0(\beta\sigma) \tag{30}$$

And C_0 is a constant. From Eq. (25), we have

$$W(p)=C_0J_0\left(\frac{\beta}{p}\right) \tag{31}$$

Based on Eqs. (20), (24) and (31) the NMR transverse magnetizations become

$$M_y(p,t)=Ae^{-(\beta^2 D/\alpha k)t}J_0\left(\frac{\beta}{p}\right)+\frac{F_o}{T_o}\int_0^t\gamma B_1(t)dt \tag{32}$$

Eq. (32) gives a single analytical expression relating the porosity, permeability, diffusion coefficient, T_1 and T_2 relaxation times and the transverse magnetization. As the situation requires, we may use Eqs. (8)–(11) to express the transverse magnetization as a function of the effective radii.

Whenever the pore volume is the same as the total volume, porosity equals 1 and since it is now nearly impossible for fluids to flow within such formations, we may sample the NMR signal such that spatial transverse magnetization from the fluids spins tends to zero. Hence, in this circumstance, we may write

$$M_{y1}(1,t)=0 \tag{33}$$

Secondly, before the introduction of the RF field, the fluid spins rotate about the B_0 field and generate extremely small transverse wave which is usually very difficult to detect (Haacke et al., 1999). If we call this a transverse magnetization component M_ρ, we then have the following initial condition:

$$(\gamma B_1=0) \tag{34}$$

From Eqs. (4), (32) and (33), we have

$$Ae^{-(\beta^2 D/\alpha k)t}J_0\left(\frac{\beta}{p}\right)=0 \tag{35}$$

Eq. (35) implies $J_0(\beta)=0$ and $\beta=\beta_1,\ \beta_2,\ \beta_3,\ldots$ are the positive roots (Kreyszig, 1996; Wylie and Barrett, 1982). Thus a solution is (Kreyszig, 1996; Wylie and Barrett, 1982)

$$M_{y1}(p,t)=Ae^{-(\beta^2 D/\alpha k)t}J_0\left(\frac{\beta_m}{p}\right);\quad m=1,\ 2,\ 3,\ldots$$

By superposition of all solutions, we write

$$M_{y1}(p,t)=\sum_{m=1}^{\infty}A_m e^{-(\beta^2 D/\alpha k)t}J_0\left(\frac{\beta_m}{p}\right) \tag{36}$$

From Eq. (34), we have

$$M_{y1}(p,0)=M_\rho(p)=\sum_{m=1}^{\infty}A_mJ_0\left(\frac{\beta_m}{p}\right) \tag{37}$$

Table 1
NMR properties of reservoir fluids (Coates et al., 1999).

Fluid	T_1 (ms)	T_2 (ms)	η[a] (cp)	$D\times10^{-5}$[b] ($cm^2\ s^{-1}$)
Brine	1–500	1–500	0.2–0.8	1.8–7
Oil	3000–4000	300–1000	0.2–1000	0.0015–7.6
Gas	4000–5000	30–60	0.011–0.014	80–100

[a] 1 cp=0.001N sm^{-2}.
[b] 1 $cm^2\ s^{-1}$=0.0001$m^2\ s^{-1}$.

Using the expressions of Eq. (25) and integration of Bessel functions (Spiegel, 1983), we write

$$A_m = \frac{2}{J_1^2(\beta_m)} \int_{\infty}^{1} \frac{1}{p^3} M_\rho(p) J_0\left(\frac{\beta_m}{p}\right) dp \tag{38}$$

If we set the magnetization component $M_\rho(p)$ to be given as

$$M_\rho(p) = -M_{\rho 0} p \tag{39}$$

then

$$M_{y1}(p,t) = \sum_{m=1}^{\infty} \left[\frac{2M_{\rho 0}}{J_1^2(\beta_m)} \int_{\infty}^{1} \frac{1}{p^2} J_0\left(\frac{\beta_m}{p}\right) dp\right] e^{-(\beta^2 D/\alpha k)t} J_0\left(\frac{\beta_m}{p}\right); \quad m = 1,\ 2,\ 3, \ldots \tag{40}$$

However,

$$\frac{2M_{\rho 0}}{J_1^2(\beta_m)} \int_{\infty}^{1} \frac{1}{p^2} J_0\left(\frac{\beta_m}{p}\right) dp = \frac{2M_{\rho 0}\left[\pi J_1(\beta_m) H_0(\beta_m) + J_0(\beta_m)\{2 - \pi J_1 H_0(\beta_m)\}\right]}{J_1^2(\beta_m)} \tag{41}$$

where $M_{\rho 0}$ is a constant and $H_n(\beta_m)$ are Struve functions of order n. Therefore, from Eqs. (32), (40) and (41), we have

$$M_y(p,t) = \sum_{m=1}^{\infty} \left\{ \frac{2M_{\rho 0}\left[\pi J_1(\beta_m) H_0(\beta_m) + 2J_0(\beta_m) - \pi J_0(\beta_m) J_1 H_0(\beta_m)\right]}{J_1^2(\beta_m)} \right\} \times e^{-(\beta^2 D/\alpha k)t} J_0\left(\frac{\beta_m}{p}\right) + \frac{F_o}{T_o} \int_0^t \gamma B_1(t) dt \tag{42}$$

Table 2
Relaxation times and relaxation rates of reservoir fluids.

Fluid	T_1 (s)	T_2 (s)	T_0 (s^{-1})	T_g (s^{-2})	T_0^2	T_0^2/T_g	T_1/T_2	T_2/T_1
Brine	0.001	0.001	2000	1,000,000	4,000,000	4	1	1
	0.25	0.25	8	16	64	4	1	1
	0.5	0.5	4	4	16	4	1	1
	0.75	0.75	2.666667	1.777778	7.111111	4	1	1
	1	0.75	2.333333	1.333333	5.444444	4.083333	1.333333	0.75
	1.25	0.75	2.133333	1.066667	4.551111	4.266667	1.666667	0.6
	1.5	0.75	2	0.888889	4	4.5	2	0.5
	1.75	0.75	1.904762	0.761905	3.628118	4.761905	2.333333	0.428571
	2	0.75	1.833333	0.666667	3.361111	5.041667	2.666667	0.375
	2.25	0.75	1.777778	0.592593	3.160494	5.333333	3	0.333333
	2.5	0.75	1.733333	0.533333	3.004444	5.633333	3.333333	0.3
	2.75	0.75	1.69697	0.484848	2.879706	5.939394	3.666667	0.272727
Oil	3	0.3	3.666667	1.111111	13.44444	12.1	10	0.1
	3.25	0.5	2.307692	0.615385	5.325444	8.653846	6.5	0.153846
	3.5	0.7	1.714286	0.408163	2.938776	7.2	5	0.2
	3.75	0.9	1.377778	0.296296	1.898272	6.406667	4.166667	0.24
Gas	4	0.03	33.58333	8.333333	1127.84	135.3408	133.3333	0.0075
	4.25	0.04	25.23529	5.882353	636.8201	108.2594	106.25	0.009412
	4.5	0.05	20.22222	4.444444	408.9383	92.01111	90	0.011111
	4.75	0.055	18.39234	3.827751	338.2783	88.37522	86.36364	0.011579
	5	0.06	16.86667	3.333333	284.4844	85.34533	83.33333	0.012

Table 3
Fluid dynamic properties, relaxation properties and corresponding transverse magnetization reservoir fluids (M_{y1} is the transverse magnetization at t=5 μs while M_{y2} is the transverse magnetization at t=5 ns; B_0=176 Gauss=0.0176 T (Coates et al., 1999)).

Fluid	T_1 (ms)	T_2 (ms)	η (N sm^{-2})	D (m^2 s^{-1})	p	k (m^2)	β	τ	r (m)	M_{y1}	M_{y2}
Brine	1	1	0.0002	1.80E−09	0.10	2.00E−15	2	6.7	1.04E−06	199.3814	5708.595
	250	250	0.0005	4.00E−09	0.11	1.02E-13	2	6.090909	6.72E−06	727.3887	823.9367
	500	500	0.0008	7.00E−09	0.12	2.02E−13	2	5.583333	8.67E−06	−5510.62	−6312.11
	750	750	0.0011	7.05E−09	0.13	3.02E−13	2	5.153846	9.78E−06	−2302.15	−2557.1
	1000	750	0.0014	7.09E−09	0.14	4.02E−13	2.020726	4.785714	1.05E−05	3741.628	3964.405
	1250	750	0.0017	7.14E−09	0.15	5.02E−13	2.065591	4.466667	1.09E−05	6915.039	7285.085
	1500	750	0.002	7.18E−09	0.16	6.01E−13	2.12132	4.1875	1.12E−05	7643.349	8006.474
	1750	750	0.0023	7.23E−09	0.17	7.01E−13	2.182179	3.941176	1.14E−05	6887.259	7182.332
	2000	750	0.0026	7.28E−09	0.18	8.02E−13	2.245366	3.722222	1.15E−05	5314.954	5520.664
	2250	750	0.0029	7.32E−09	0.19	9.01E−13	2.309401	3.526316	1.16E−05	3335.235	3448.28
	2500	750	0.0032	7.37E−09	0.2	1.00E−12	2.373464	3.35	1.16E−05	1198.111	1221.951
	2750	750	0.0035	7.41E−09	0.21	1.10E−12	2.437087	3.190476	1.16E−05	−947.498	−1005.98
Oil	3000	300	0.0038	7.46E−09	0.22	1.20E−12	3.478505	3.045455	1.15E−05	−37892.8	−40659.7
	3250	500	0.0041	7.51E−09	0.23	1.30E−12	2.941742	2.913043	1.15E−05	10900.15	11400.75
	3500	700	0.0044	7.55E−09	0.24	1.40E−12	2.683282	2.791667	1.14E−05	−5183.19	−5394.24
	3750	900	0.0047	7.60E−09	0.25	1.50E−12	2.531139	2.68	1.13E−05	−8672.6	−8960.26
Gas	4000	30	0.000011	8.00E−08	0.26	1.60E−12	11.63361	2.576923	1.13E−05	27.31702	2346.491
	4250	40	0.00001175	8.50E−08	0.27	1.70E−12	10.40478	2.481481	1.12E−05	412.7572	59278.35
	4500	50	0.0000125	9.00E−08	0.28	1.80E−12	9.592242	2.392857	1.11E−05	−46.1217	−6070.9
	4750	55	0.00001325	9.50E−08	0.29	1.90E−12	9.400809	2.310345	1.10E−05	178.8574	8488.154
	5000	60	0.000014	1.00E−07	0.30	2.00E−12	9.238254	2.233333	1.09E−05	64.99404	1127.022

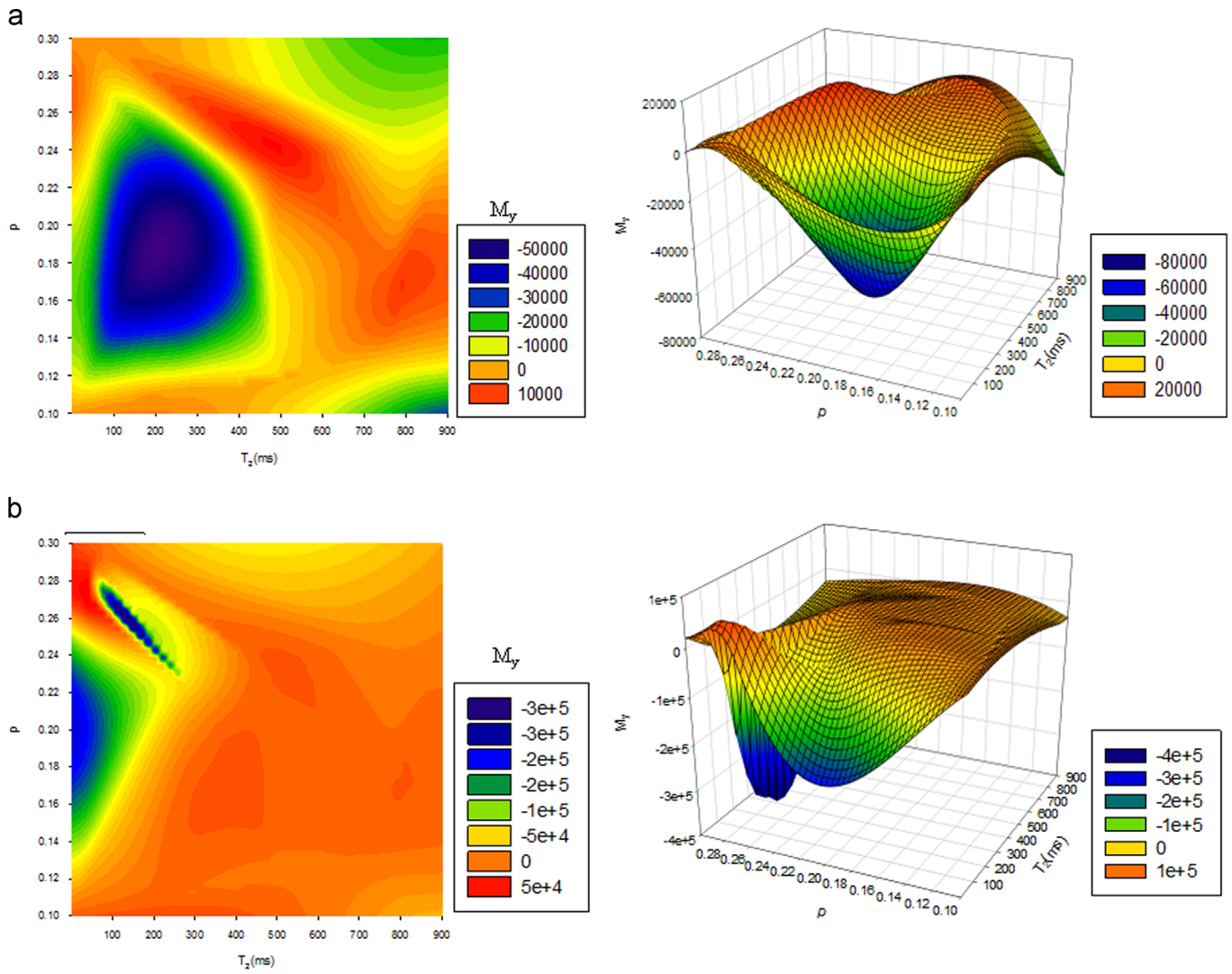

Fig. 2. Contour maps and 3D plots of transverse magnetization as it varies with T_2 and porosity, p at (a) t=5.0 μs and (b) t=5.0 ns.

3. Analysis of results

The NMR signal as given in Eq. (42) is dependent on the nature of the RF field. If we assume the RF field is given as follows (Awojoyogbe et al., 2013):

$$\gamma B_1(t) = \gamma G(t) r \tag{43}$$

The integral in Eq. (42) becomes

$$\frac{F_o}{T_o}\int_0^t \gamma B_1(t)dt = \gamma M_0 r \frac{1}{T_1 T_0}\int_0^t G(t)dt \tag{44}$$

If we further assume that the gradient pulse $G(t)$, is designed such that $G(t)$ undergoes exponential rise and fall, we may write (Price, 1997, 1998):

$$G(t) = ge^{-kt} \tag{45}$$

where k is the exponential rate constant (Price, 1998). If we set $k=(T_g/T_0)$ and the integral in Eq. (44) has a new lower limit as the gradient pulse time δ, we obtain

$$\frac{F_o}{T_o}\int_\delta^t \gamma B_1(t)dt = -\frac{M_0\gamma g r}{T_1 T_g}e^{-(T_g/T_0)(t-\delta)} = -(M_0 T_2 \gamma g r)e^{-(T_g/T_0)(t-\delta)} \tag{46}$$

Therefore, Eq. (42) becomes

$$M_y(p,t) = \sum_{m=1}^{\infty}\left\{\frac{2M_{\rho 0}[\pi J_1(\beta_m)H_0(\beta_m)+2J_0(\beta_m)-\pi J_0(\beta_m)J_1H_0(\beta_m)]}{J_1^2(\beta_m)}\right\} \times e^{-(\beta^2 D/\alpha k)t}J_0\left(\frac{\beta_m}{p}\right) - \{M_0 T_2 \gamma g r\}e^{-(T_g/T_0)(t-\delta)} \tag{47}$$

Eq. (47) is the analytical expression for the porosity-dependent transverse magnetization describing NMR signal in reservoir rocks.

The NMR properties of different reservoir fluids are very different from one another (Coates et al., 1999). The consequence of these differences is that it is possible to accurately describe hydrocarbons and quantify their volumes. For this reason, we shall analyse our results with NMR features of brine, oil and gas as given below (Coates et al., 1999):

Using the results in Eqs. (42) and (47) and relaxation parameters in Table 1, we have Tables 2 and 3:

Diffusion coefficient represents the proportionality constant between the molar flux due to molecular diffusion and the gradient in the concentration of the pore fluids. It is a very useful hydrodynamic property of reservoir fluids which is important in the characterization of such fluid. Table 1 presents diffusion coefficients of bulk fluids (brine, oil, and gas) at reservoir conditions using Magnetic Resonance Imaging Logging (MRIL) measurements (Coates et al., 1999).

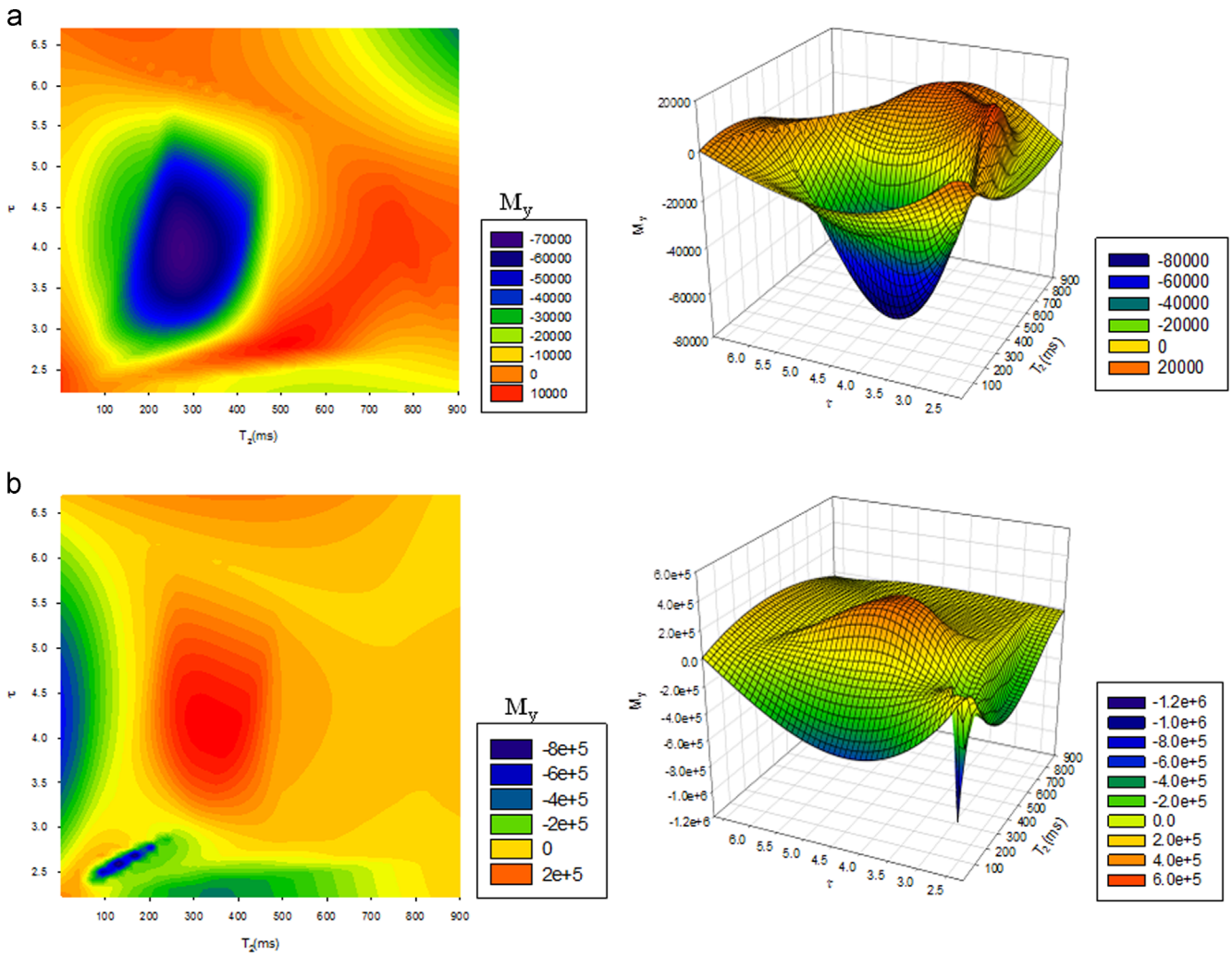

Fig. 3. Contour maps and 3D plots of transverse magnetization as it varies with T_2 and tortuosity, τ at (a) $t=5.0$ μs and (b) $t=5.0$ ns.

In the construction of Tables 2 and 3, we have used the following parameters within the computations: $B_0=0.0176$ T, $M_0=8.0$ A m^{-1}, $G=0.2$ T m^{-1}, $\delta=0.002$ s. Using the values in Table 3, we have made the following plots in Figs. 2–9.

4. Discussion

Figs. 2–5 show the maps of the transverse magnetization as the relaxation time T_2, and hydrodynamic parameters of reservoir fluids change. Each of these figures shows that reservoir NMR mapping could be done when the values of only one or very few hydrodynamic features are known. However, the choice of hydrodynamic parameter may depend on the kind of information the petro-physicist is seeking. Fig. 2 shows the transverse magnetization maps of a reservoir containing brine, oil and gas flowing in rocks of different porosities. It would be observed that the maps do not show sharp changes between the fluids but rather, the contours slowly transform their values of M_y. This shows that the fluids are not always distinct at every region but exist as a mixture of varying compositions. Fig.1b shows that some hidden features in Fig. 2a could be seen if we use very small sampling time. Particularly, the unique small blue region shows gas features with extended tail; which may be gas mixed with other fluids. It is also worthy of note that the negative values of M_y may signify the presence of electron resonance signals.

Tortousity is a measure of how twisted porous media are. We may regard this as a measure of complexities in rock pore connections. This description fits into complex lithologies so that once we are able to measure the tortuosity of the reservoir; the results obtained could be used to evaluate NMR signals for different fluids. Fig. 3b also reveals hidden features of Fig. 3a. The same unique blue region still appeared below at the point where the tortuosity is very low. Figs. 4 and 5 show the influence of fluid properties on the signals.

Figs. 6–9 are very informative, straightforward and self-explanatory. The fluids show unique curves at different sampling times; showing unique transverse magnetization. This may prove to be very important in NMR spectroscopic studies of petroleum reservoirs.

The criteria for detecting the difference in oil, brine and gas are the parameters (e.g. porosity and T_2) on the axis of Figs. 2–9. A combination of these parameters corresponds to inter-fluid contrast. As seen on the maps and plots, the computational results in this study give the opportunity of intra-fluid contrast. This is especially useful for fluids flowing from one region of reservoir rock to another with different porosity values. T_2 changes are synonymous to molecular interaction which the fluids participate in; and they are consequences of fluid composition and other fluid properties (such as temperature and pressure). These results make it possible to map NMR signals of

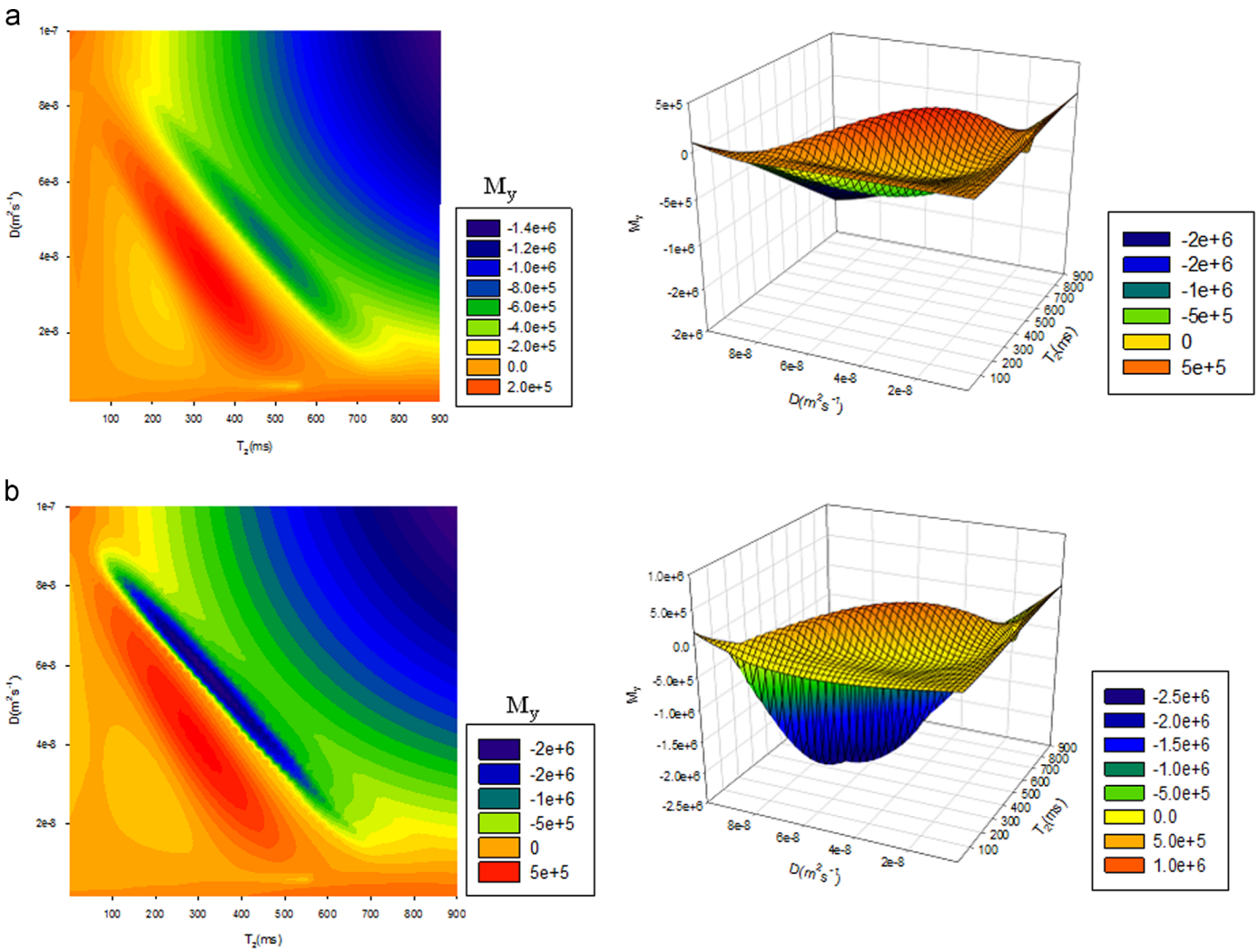

Fig. 4. Contour maps and 3D plots of transverse magnetization as it varies with T_2 and diffusion coefficient, D at (a) $t=5.0$ μs (b) $t=5.0$ ns.

specific reservoir physical feature (like porosity) and chemical properties (molecular interactions). An interesting feature on these illustrations is the fading colour maps whose values are naturally non-existent in experimental data but have been extrapolated from known experimental values (Mitchell et al., 2013; Coates et al., 1999). With this, it is possible to run several values for successful job planning. This can reduce data processing time and gives experimental scientists a computing tool with which they could run data sets which may not be allowed by the hardware setup of the NMR logging machine.

Porosity is a measure of the volume allowed for the fluids within a rock sample and tortuosity describes how complex and twisted the pores are. Mapping the transverse magnetization M_y to these parameters may lead to new understanding of fluid behaviour in pore spaces. Some fluid properties originate from quantum behaviour of atoms of the fluids; at large sampling time, their behaviour could have dissolved into bulk macroscopic behaviour. Mapping at smaller sampling time allows us to observe changes that disappear or become blurred at larger sampling time.

It is known that diffusion coefficient indirectly quantifies the adhesive force between the fluids and pore spaces. Hence, the NMR signal is particularly sensitive to the diffusion coefficient measurement of oil and gas but does not lead to impressive signal in gas. This shows that the results in this study are sensitive to processes leading to and sustaining wettability.

5. Conclusion

We have solved the Bloch NMR flow equations for the analysis of fluid flow dynamics applicable in petroleum-bearing reservoirs and complex mineralogy earth formations. It is shown that reservoir NMR mapping could be done when the values of only one or very few hydrodynamic features are known. The choice of hydrodynamic parameter may depend on the kind of information required. It is demonstrated that the measured tortuosity of the reservoir could be used to evaluate NMR signals for different fluids. The unique NMR transverse magnetization obtained at different sampling times may prove to be very important in NMR spectroscopic studies of petroleum reservoirs.

It is quite known that NMR is already used in various core analysis laboratories to characterize rocks and fluids, obtain pore-size distribution, determine porosity and even evaluate rock wettability qualitatively using different numerical methods. Also, NMR contrasts due to rock geochemical and morphological effects from the intrinsic fluid effects is the main emphasis today for NMR petrophysicist – to quantify saturating fluids and to assess the reservoir quality. A major contribution of this study is the development of a single analytical expression relating the porosity, permeability, diffusion coefficient, T_1 and T_2 relaxation times and the transverse magnetization as shown in Eq. (32). Eq. (47) is the

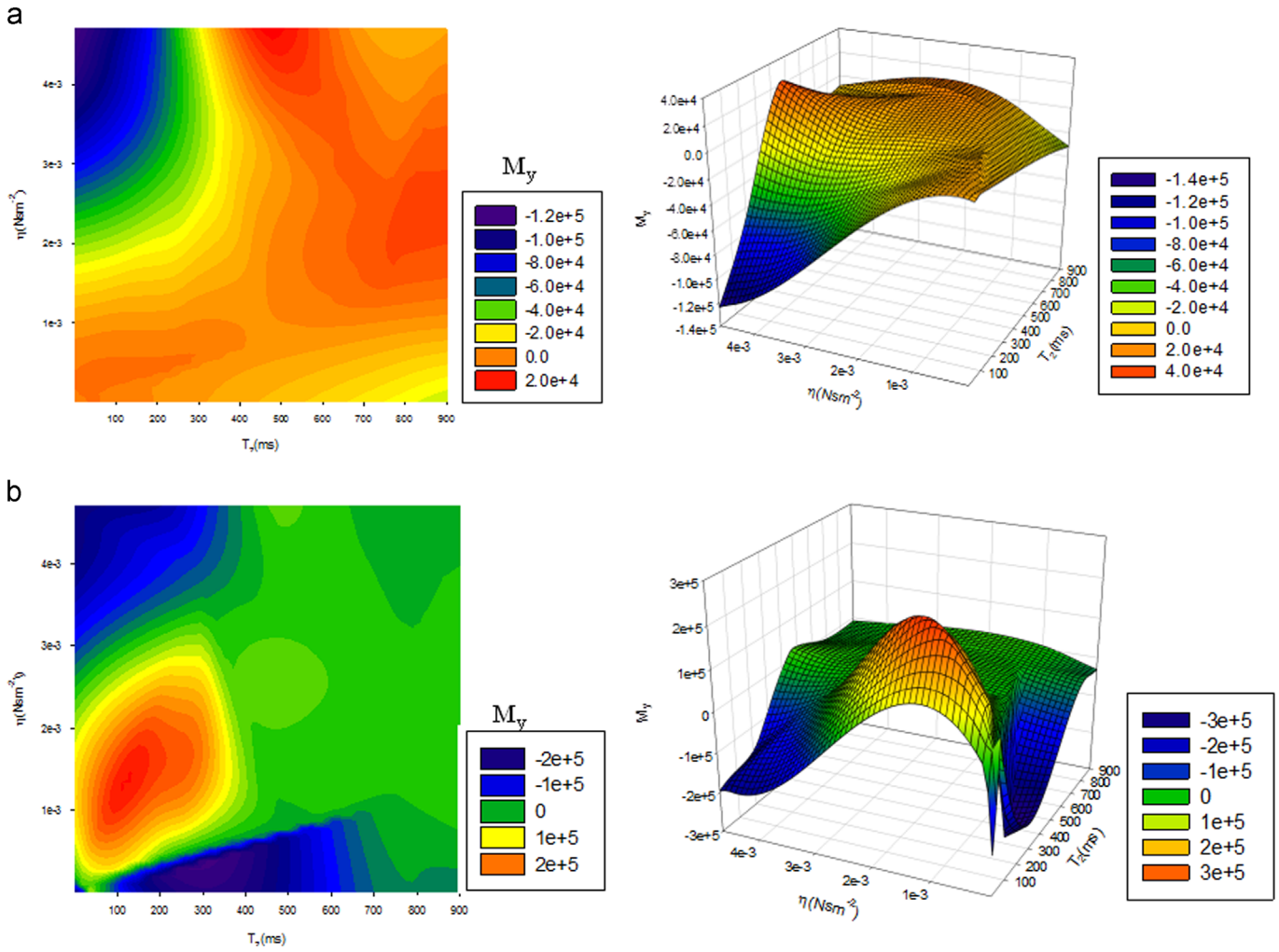

Fig. 5. Contour maps and 3D plots of transverse magnetization as it varies with T_2 and viscosity, η at (a) t=5.0 μs (b) t=5.0 ns.

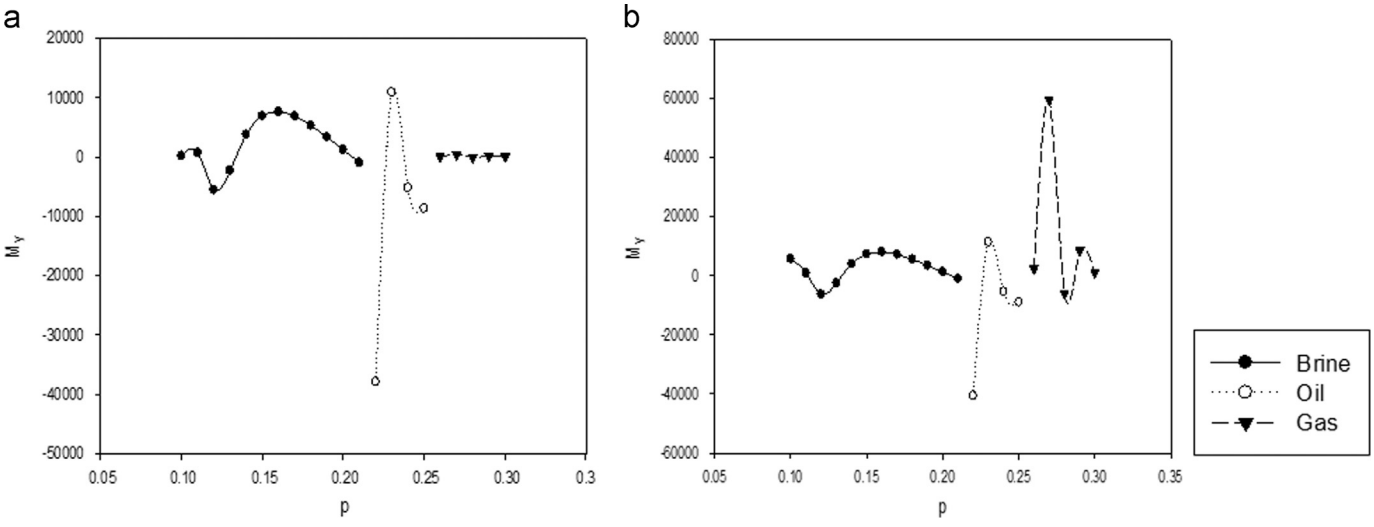

Fig. 6. Plot of transverse magnetization against porosity, p at (a) t= 5.0 μs (b) t=5.0 ns.

analytical expression for the porosity-dependent transverse magnetization describing NMR signal in reservoir rocks. This would significantly enhance the present understanding for quantitative evaluation of rock wettability, particularly for cases where oil and brine T_2 relaxation times/peaks are close as illustrated in Figs. 5–8. It can also be used to visualize and track the saturation front during displacement experiments (dynamic measurements). This will be the focus of our next investigation. The difficulty in

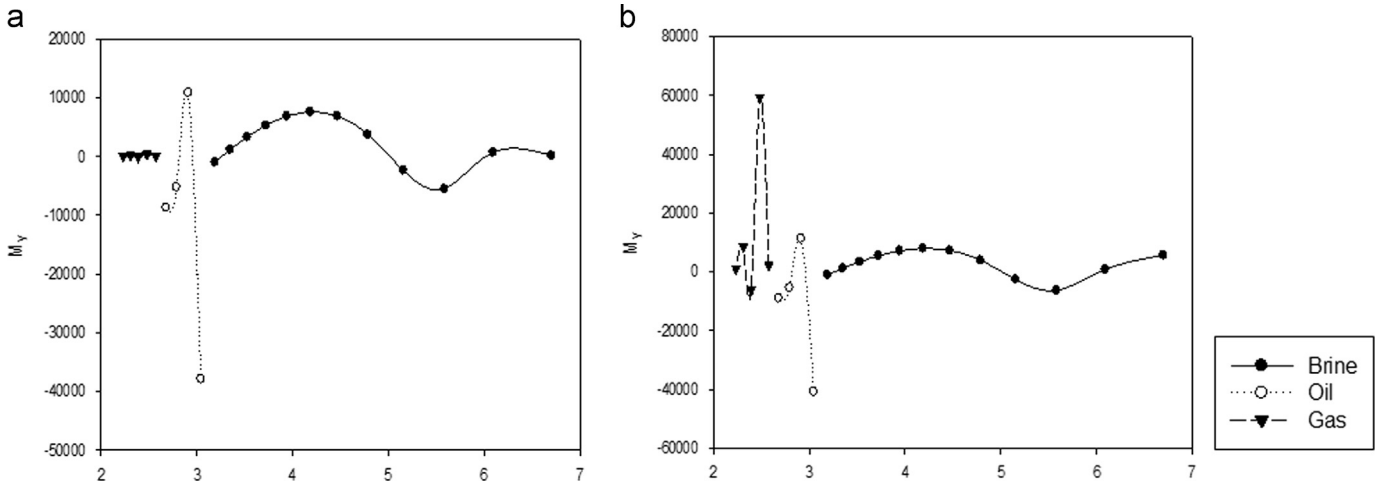

Fig. 7. Plot of transverse magnetization against tortuosity, τ at (a) $t=5.0$ μs (b) $t=5.0$ ns.

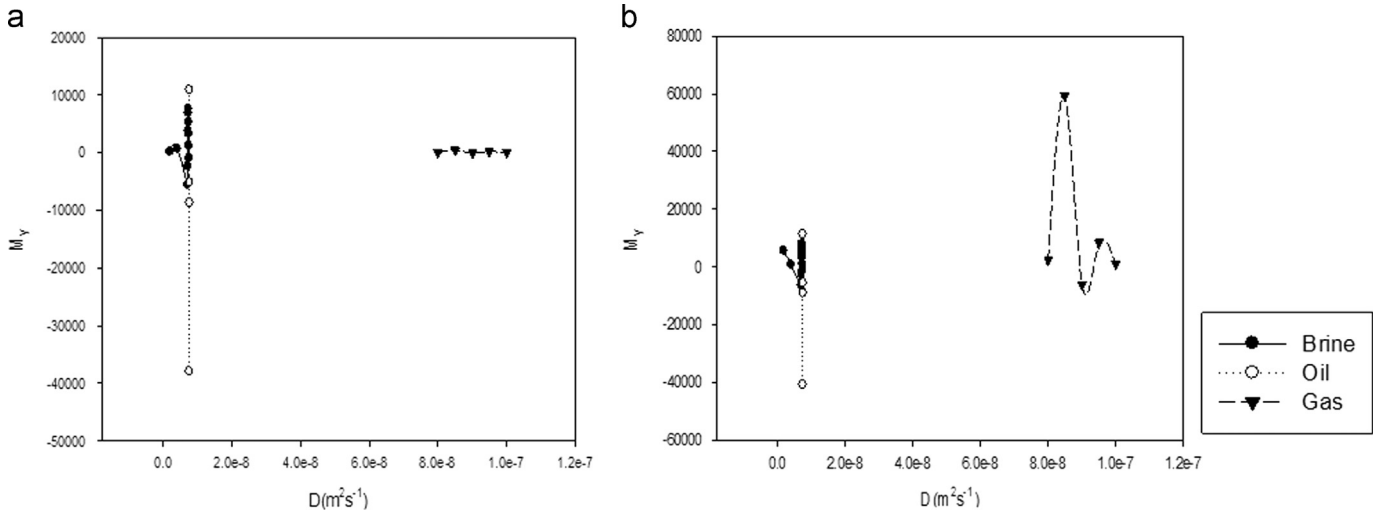

Fig. 8. Plot of transverse magnetization against diffusion coefficient, D at (a) $t=5.0$ μs (b) $t=5.0$ ns.

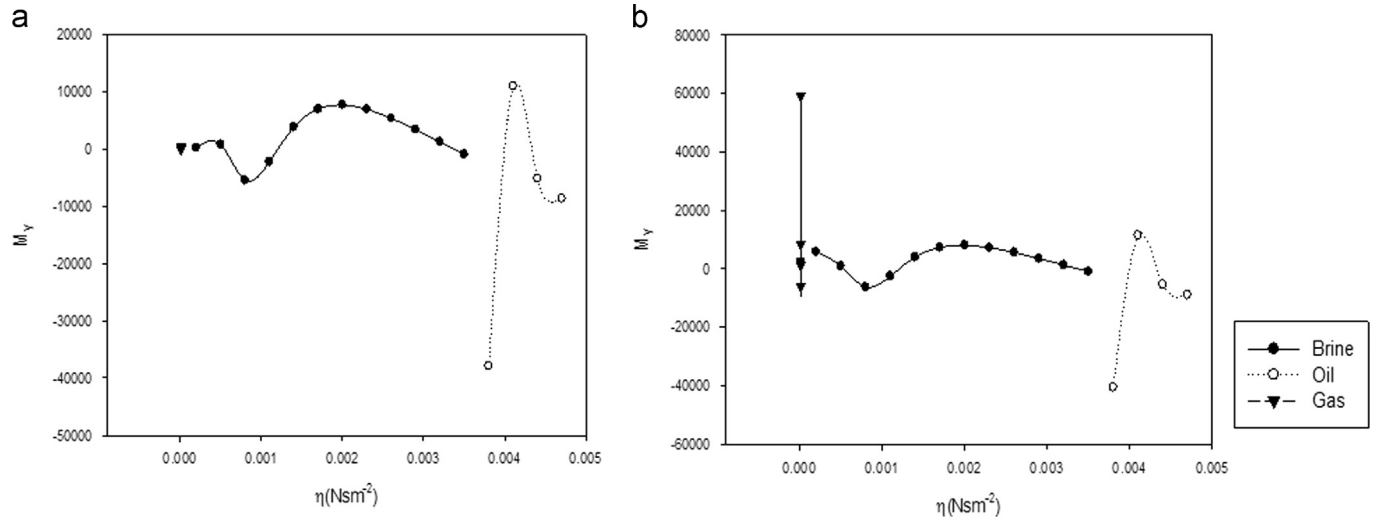

Fig. 9. Plot of transverse magnetization against viscosity, η at (a) $t=5.0$ μs and (b) $t=5.0$ ns.

estimating permeability from grain-size distributions or from well logs can be reduced very significantly by the simple relationships between permeability, porosity and tortuosity assumed to achieve the analytical solution in Eqs. (32) and (47) respectively.

References

Awojoyogbe, O.B., Dada, M., 2011. The dynamics of NMR-diffusion equation for the analysis of hemodynamic and metabolic changes in biological tissue.

In: Emma T., Berg (Ed.), Fluid Transport: Theory, Dynamics and Applications. Nova Science Publication, USA, ISBN: 978-1-61122-317-0, ISBN-10: 1611223172.
Awojoyogbe, O.B., Faromika, O.P., Folorunsho, O.M., Dada, M., Fuwape, I.A., Boubaker, K., 2010. Mathematical model of the Bloch NMR flow equations for the analysis of fluid flow in restricted geometries using the Boubaker polynomials expansion scheme. Curr. Appl. Phys. 10, 289–293.
Awojoyogbe, O.B., Dada, O.M., Faromika, O.P., Dada, O.E., 2011. Mathematical concept of the Bloch flow equations for general magnetic resonance imaging: a review. Concepts Magn. Reson. Part A 38A (3), 85–101.
Awojoyogbe, O.B., Dada, M., Boubaker, K., Adesola, O.A., 2013. Flow dynamics in restricted geometries: a mathematical concept based on Bloch NMR flow equation and Boubaker Polynomial Expansion Scheme. J. Appl. Math. Phys. 1, 71–78.
Chen, S., Li, L., Zhang, G., Chen, J., 2011. Magnetic resonance for downhole complex-lithology earth formation evaluation. New J. Phys. 13, 085015.
Coates, G.R., Xiao, L., Prammer, G.M., 1999. NMR Logging Principles and Applications. Halliburton Energy Services, Houston, USA.
Freedman, R., Heaton, N., 2004. Fluid characterization using nuclear magnetic resonance logging. Petrophysics 45 (3), 241–250.
Gupta, A., Stait-Gardner, T., Ghadirian, B., Price, W.S., Dada, O.M., Awojoyogbe, O.B., 2014. Theory, Dynamics and Applications of Magnetic Resonance Imaging—I. Science Publishing Group, New York, USA.
Haacke, M.E., Brown, R.W., Thompson, M.R., Venkatesan, R., 1999. Magnetic Resonance Imaging: Physical Principles and Sequence Design. John Wiley and Sons, New York, pp. 39–49.
Howard, J.J., 1998. Quantitative Estimates of Porous Media Wettability from Proton NMR Measurements. Magn. Reson. Imaging 16 (5/6), 529–533.
Kleinberg, R.L., Kenyon, W.E., Mitra, P.P., 1994. Mechanism of NMR Relaxation of Fluids in Rocks. J. Magn. Reson. 108, 206–214.
Kreyszig, E., 1996. Advanced Engineering Mathematics, Seventh edition John Wiley & Sons, Singapore.
Mitchell, J., Chandrasekera, T.C., Holland, D.J., Gladden, L.F., Fordham, E.J., 2013. Magnetic resonance imaging in laboratory petrophysical core analysis. Phys. Rep. 526 (3), 165–225.
Morriss, C.E., Freeman, R., Straley, C., Johnston, M., Vinegar, H.J., Tutunjian, P.N., 1994. Hydrocarbon saturation and viscosity estimation from NMR logging in the Belridge Diatomite. In: Transactions of the SPWLA 35th Annual Logging Symposium. Tulsa, Oklahoma, USA. June 19–22 (paper C).
Pape, H., Clauser, C., Iffland, J., 1998. Permeability Prediction for reservoir sandstones and basement rocks based on fractal pore space geometry. SEG Expand. Abstr.
Price, W.S., 1997. Pulsed field gradient nuclear magnetic resonance as a tool for studying translational diffusion: Part I. Basic theory. Concepts Magn. Reson 9, 299–336.
Price, W.S., 1998. Pulsed-field gradient nuclear magnetic resonance as a tool for studying translational diffusion: Part II. Experimental aspects. Concepts Magn. Reson. 10 (4), 197–237.
Sen, P.N., 2004. Time-dependent diffusion coefficient as a probe of geometry. Concepts Magn. Reson. Part A 23 (1), 1–21.
Spiegel, MR., 1983. Schaum's Outline Series of Theory and Problems of Advanced Mathematics for Engineers and Scientists. McGraw-Hill, Singapore.
Wylie, C.R., Barrett, C.L., 1982. Advanced Engineering Mathematics. McGrawl-Hill, Tokyo, Japan.